Objective Identification of Tornado Seasons and Ideal Spatial Smoothing Radii

P. Grady Dixon,* Andrew E. Mercer, Katarzyna Grala, and William H. Cooke

Department of Geosciences, Mississippi State University, Mississippi State, Mississippi

Received 11 September 2013; accepted 25 November 2013

ABSTRACT: The fundamental purpose of this research is to highlight the spatial seasonality of tornado risk. This requires the use of objective methods to determine the appropriate spatial extent of the bandwidth used to calculate tornado density values (i.e., smoothing the raw tornado data). With the understanding that a smoothing radius depends partially upon the period of study, the next step is to identify objectively ideal periods of tornado analysis. To avoid decisions about spatial or temporal boundaries, this project makes use of storm speed and tornado pathlength data, along with statistical cluster analysis, to establish tornado seasons that display significantly different temporal and spatial patterns. This method yields four seasons with unique characteristics of storm speed and tornado pathlength.

The results show that the ideal bandwidth depends partially upon the temporal analysis period and the lengths of the tornadoes studied. Hence, there is not a ''one size fits all,'' but the bandwidth can be quantitatively chosen for a given dataset. Results from this research, based upon tornado data for 1950–2011, yield ideal bandwidths ranging from 55 to 180 km. The ideal smoothing radii are then applied via a kernel density analysis of each new tornado season.

KEYWORDS: Tornadoes; Statistical climatology; Spatial analysis

* Corresponding author address: P. Grady Dixon, Department of Geosciences, Mississippi State University, Mississippi State, MS 39762-5448.

E-mail address: grady.dixon@msstate.edu

DOI: 10.1175/2013EI000559.1

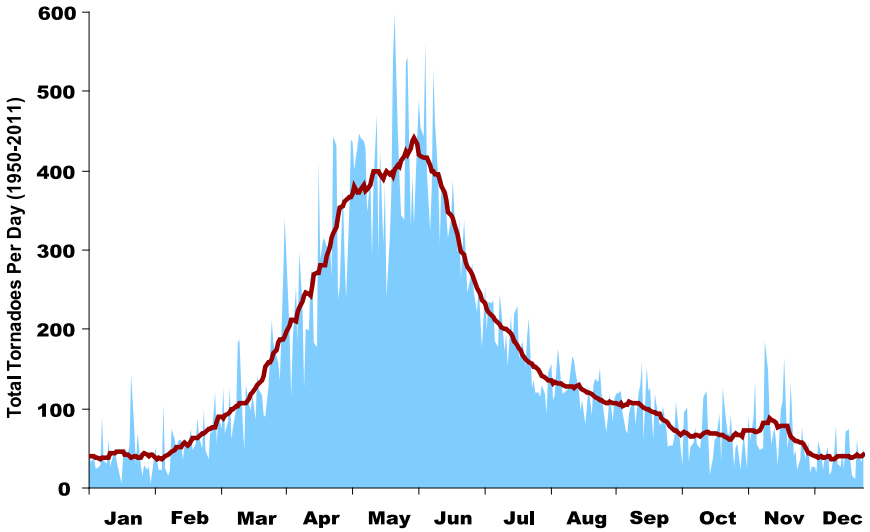

Figure 1. Total number of U.S. tornadoes (1950–2011) by day of the year. The dark red line is a 21-day moving average.

1. Introduction

Tornado climatology research in the United States has shown that subjective and sometimes arbitrary decisions must be made when deciding what types of temporal and/or spatial bounds to apply to the data. Some studies include all events (Thom 1963; Kelly et al. 1978; Schaefer et al. 1986; Brooks et al. 2003; Dixon et al. 2011), while others analyze only killer (Boruff et al. 2003; Ashley 2007) or strong/long-track tornadoes (Concannon et al. 2000; Broyles and Crosbie 2004; Guyer et al. 2006; Kis and Straka 2009). Likewise, many studies are restricted to specific, predetermined areas (Emery 1900; Hanstrum et al. 2002; Guyer et al. 2006; Gagan et al. 2010) or times (Hanstrum et al. 2002; Guyer et al. 2006; Ashley et al. 2008; Kis and Straka 2009).

These decisions to reduce the total sample size are made for good reasons that are often associated with testing specific hypotheses but, even when the total sample of recorded tornado events is used, there may not be enough statistical power to draw many conclusions about temporal and spatial patterns (Doswell 2007). Most researchers employ spatial smoothing techniques to overcome some of the problems associated with an incomplete and inconsistent dataset; however, there is no clear "best" shape or size for smoothing methods (Dixon and Mercer 2012; Marsh and Brooks 2012).

The variety of decisions made by researchers suggests that there is also no singular best method for identifying temporal or spatial delimiters of tornado data. The idea of a "tornado season" is a good example of this problem. Figure 1 suggests that the peak in tornado frequency is in late spring (i.e., late May) and that there are as many tornadoes or perhaps more throughout the summer (June–August) as there are in the spring (March–May). If we reproduce Figure 1 for smaller subsections of the total sample (specific intensities, areas, times of day, etc.), the graph will likely appear substantially different, as shown by Brooks et al. (2003).

The purpose of this study is to create seasonal tornado risk maps for the United States. This goal requires the use of objective methods to identify the appropriate distance parameter for depicting tornado frequency using a geographical information system (GIS)-based kernel density analysis function and to apply this function to objectively identified seasons of tornado activity. GIS density analysis functions and similar smoothing techniques have been frequently used to illustrate the density or probability of tornadoes and tornado-related variables (Thom 1963; Kelly et al. 1978; Schaefer et al. 1986; Concannon et al. 2000; Brooks et al. 2003; Ashley 2007; Dixon et al. 2011; Dixon and Mercer 2012; Marsh and Brooks 2012). However, these analyses have typically been applied without quantitative evidence for decision processes associated with selecting the appropriate spatial analysis extent, temporal analysis period, and appropriate tornado pathlength.

1.1. Identifying appropriate radii for smoothing tornado data

Aggregation of tornado events into temporal and/or spatial groups suggests that the events are related (correlated) in time and/or space. The term ‘‘spatial autocorrelation’’ is derived from time series analysis and is most closely associated with the univariate statistics notion of correlation (de Smith et al. 2007). Various measures of spatial autocorrelation have been used to assess the presence of spatial stability (i.e., consistent values across space) within a dataset. Spatial stability may be common at some scales, but it is expected to diverge toward spatial heterogeneity (also referred to as spatial nonstationarity) at other scales (Anselin 1995; Anselin 1996). The global Moran’s I index (referred to only as Moran’s I) is one method for quantifying spatial stability, where the calculated index value I is most commonly applied to measure spatial autocorrelation for areal units (e.g., tornado pathlengths) that are numerical ratio or interval data (O’Sullivan and Unwin 2003). Moran’s I is often used to explore spatial clustering upon the landscape, providing indications of underlying spatial processes (Santamaría et al. 2007; Mitchell and Powell 2008; Nelson and Boots 2008; Portnov et al. 2009; Willems and Hill 2009). The kernel radius (commonly referred to as the bandwidth) that exhibits maximum clustering, as measured by Moran’s I, is the distance where those spatial processes are most pronounced (Fortin et al. 2006). Hence, Moran’s I was used as a bivariate regression coefficient to determine the extent to which neighboring tornado pathlengths vary together (i.e., are correlated) over a variety of distances to identify the minimum (i.e., ideal) bandwidth necessary to maximize spatial stability.

1.2. Delineating tornado seasons

A simple count of tornado frequency across the study area is a common first step in determining questions about seasonality, yet decisions must be made almost immediately regarding spatial and temporal scales. Greater spatial resolution reduces the number of events within each spatial unit (i.e., a decreased sample size at all locations), so a strong argument can be made in support of coarser spatial and temporal resolutions. These types of coarse analyses have produced broad conclusions such as ‘‘tornadoes are most common in the spring’’ or ‘‘Texas experiences the most tornadoes.’’ At some scale, these statements are true and valuable to

the public, but they are certainly not applicable for all times or places in the United States. Knowing when and where the most tornadoes occur is important, but such counts can be misleading in efforts to understand risk, mitigate damage, and prepare for impacts as numerous short-path tornadoes may not cover as much cumulative ground or affect as many people as a few tornadoes with longer paths. Therefore, the methods used here are focused on storm speed and tornado pathlengths to effectively capture the seasonal risks to life and property.

Initial attempts to identify objectively the appropriate smoothing radius for tornado density analyses yielded results suggesting that the ideal bandwidth depends partially upon the temporal analysis period and the lengths of the tornadoes in the sample. Therefore, various tornado seasons should be delineated according to timing and tornado length characteristics. There are two primary factors that determine the length of a tornado: the speed and duration. Previous research suggests that strong tornadoes tend to last longer than weak tornadoes or at least be associated with longer-lasting mesocyclones (Wood et al. 1996), so using duration in our analyses would likely create a bias toward strong events. Conversely, storm speed does not necessarily increase with tornado intensity (Wood et al. 1996), so storm speed is included in our analysis along with tornado pathlength and day of the year (DOY) to delineate separate seasons of tornado characteristics objectively.

2. Methods

2.1. Tornado path data

This project makes use of the complete available tornado record (1950–2011) compiled by the National Weather Service Storm Prediction Center (SPC). Previous researchers have detailed the dataset (Schaefer and Edwards 1999; McCarthy 2003) and many of the issues associated with it (Doswell and Burgess 1988; Brooks et al. 2003; Brooks 2004). One of the biggest concerns with this dataset, for the purposes of this research, is the inconsistency between reported tornado lengths and the path coordinates. Of the 56 000+ tornadoes in the dataset, only 119 have reported lengths of zero and only 396 have reported lengths of 100 m or less. However, there are more than 35 000 tornadoes with identical starting and ending coordinates (latitude, longitude). Point-touchdown records will result in exponentially smaller density values than paths at small scales, so the coordinates must be edited to provide an improved estimate of actual tornado pathlengths.

One possible way to assign realistic pathlengths to events without ending coordinates is to assign an ending location that achieves a distance equivalent to the distance reported by the ‘‘length’’ variable in the dataset. Unfortunately, there are two significant problems with this strategy. First, there is no way to know the direction of the path. Second, many of the reported length values are surprisingly large (the largest is 129 km), so applying that length in an arbitrary direction would likely create a false impact upon numerous communities. It is unlikely that a tornado could travel that far and not have an official terminus, and it is more probable that there is an error in the database in such cases.

For the justification of these methods, it is important to note that the tornado database lists pathlengths in miles. Among the tornado records that lack official ending locations, by far most of them (15 432) have lengths of 0.1 mi or less. The

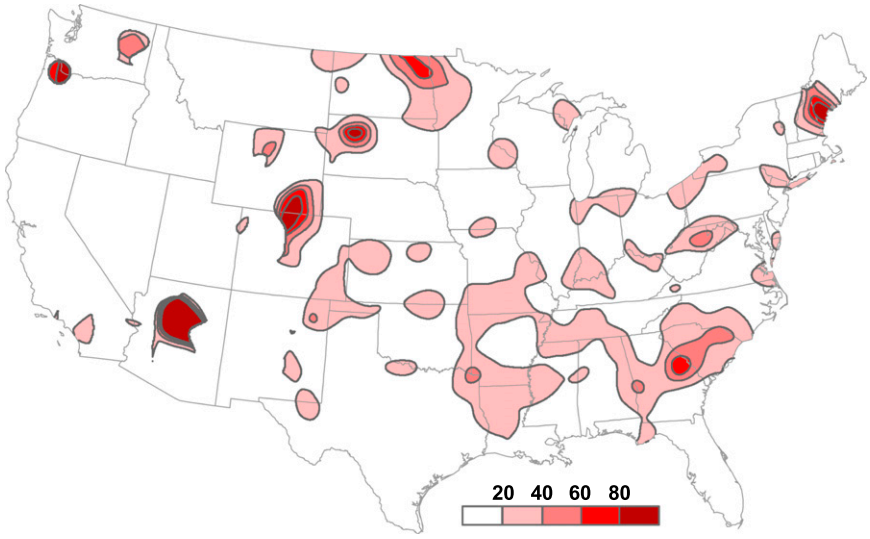

Figure 2. Percent increase in annual tornado density (in km of tornado path within 40 km of a point) resulting from the addition of 0.1 km of pathlength to points without terminus coordinates. Areas were excluded from the calculation if their original density was less than 0.1 to reduce "noise" in areas with very low tornado path densities.

next two most common values are 0.5 and 0.2 mi, with 4333 and 4229 reports, respectively. Approximately 80% of these records show lengths of 0.5 mi or less, so it is probable that all tornadoes without ending locations are short-path events and it is very likely that length values of "0.1 mi" have been approximated rather than measured. Therefore, for the purpose of this study, all events without terminus location coordinates are considered to have pathlengths of 0.1 km. Each of the events in question will have an ending coordinate created that is 0.1 km due north of the initial location, which can result in substantial density increases in a few areas (Figure 2). Nearly 70% of the tornadoes with official termination points displayed path directions of 0°–60° (i.e., toward the north or northeast), but a northward addition was chosen for simplicity. The direction is insignificant because of the very small length added and the smoothing of the kernel density analysis applied later. Therefore, areas affected by this change will see increases in density values regardless of the direction of the added pathlengths. The purpose of this approximation is to ensure that the numerous tornado events with incomplete path information are better represented in the analyses. As most previous studies have ignored this issue, this method should yield a more favorable representation of these events.

2.2. Tornado speed data

There is no official dataset that includes tornado speed. However, the text of tornado warnings have been archived for several years, and nearly all tornado

warnings include an assessment of storm speed. Because one objective of this project is to identify tornado seasons based on speed and pathlength, archived tornado warnings were used as a proxy for actual tornado speed information. This assumes that there is a seasonality to storm speed such that a sample of storm speeds from archived warnings is reasonably representative of typical tornado speeds for that time of year. Given the high probability of errors associated with warning speeds and/or direction for any single tornado event, it is important to understand that there are several limitations associated with using tornado warnings as representations of actual tornado speeds. Nevertheless, the purpose of this method is to approximate the typical speed of tornado-producing thunderstorms so that differences can be delineated for various times of the year. This means that accuracy is not as important as consistency, and the large number of warnings (46 175) should provide a representative sample despite the errors likely to be present in any individual records. Tornado warning text was acquired from the National Climatic Data Center for April 2001 through August 2012 (the full period of record).

2.3. Tornado seasons identification

Average pathlengths for each day of the year were determined using the SPC tornado database. Storm speeds, based on warning data from 2001 to 2012, were divided into categories of slow (10th percentile), intermediate (middle 80th percentile), and fast (90th percentile). These equated to values of less than 25 km h^{-1} (15 mph), 25–80 km h^{-1} (15–50 mph), and greater than 80 km h^{-1} (greater than 50 mph), respectively. To account for differences in the number of total warnings issued for each day, percentages of slow, intermediate, and fast storms were calculated for each day of the year. A 21-day moving average was then applied to the daily percentages. Daily average pathlength and the three daily percentages were all included in a statistical *K*-means cluster analysis (Wilks 2006). A *K*-means cluster analysis requires a rather subjective selection of the number of clusters to be used in the analysis. Therefore, an initial test with three clusters was used to identify seasons based on tornado characteristics. Another analysis was performed using four clusters to determine whether more seasons would improve upon any possible ambiguity present in the first analysis.

2.4. Global Moran's I calculation

Spatial autocorrelation analysis was performed by segmenting the tornado data (1950–2011) according to season, as established from the methods in section 2.3, and then calculating global Moran's I. To ensure that calculations are based on the most tornado-prone regions of the United States, analyses were restricted to locations east of 105°W longitude (similar to Marzban and Schaefer 2001). A series of Moran's I calculations were run for multiple bandwidths to select those that reflect maximum spatial autocorrelation in the tornado data. Moran's I values near 1.0 are associated with clustering of like values (i.e., spatial autocorrelation), values near −1.0 are associated with dispersion of like values, and values near 0 suggest no spatial autocorrelation (Sheppard et al. 2007).

Table 1. Results of cluster analysis using pathlengths and percentages of storm-speed categories for each day of the year.

Cluster periods (DOY)	Season name	Start date
26–72	Winter	26 Jan
73–127	Spring	14 Mar
128–288	Summer	8 May
289–25	Fall	16 Oct

Two methods were used to determine which data were included in each calculation of Moran's I. The first simply uses the tornado seasons established in the first part of the research. Hence, all tornadoes east of 105°W were included if they occurred during the season in question. This yields a different ''ideal'' bandwidth for each season. This analysis was also performed using only tornado initiation points for the purpose of future studies that are more interested in tornadogenesis rather than tornado paths and impacts.

The second method restricts the spatial analysis of each season to those states with the greatest tornado density. Moran's I cannot be calculated at radii smaller than the distance between any two points, so spatial outliers have the potential to control the minimum acceptable bandwidth rather than characteristics of the most tornado-prone regions. For each season, states were included in the analysis if significant portions of the state displayed density values (calculated using radii in the first method) similar to the core of greatest density. This was generally consistent with any state that experienced continuous areas with at least 0.10 km of tornado path per year within 40 km of a point. For winter, the density values are much lower, so states were chosen if more than half of their area experienced at least 0.05 km of tornado path per year within 40 km of a point.

To determine spatial autocorrelation (i.e., Moran's I), there must be at least one variable, in addition to location, that is compared to other locations. Otherwise, it is an assessment of pure clustering rather than spatial autocorrelation (i.e., similar events or features). For this study, spatial autocorrelation is determined by comparing all tornado paths that fall at least partially within the radius of analysis according to their total lengths.

Z scores were calculated for each run of the analysis to provide a measure of statistical significance such that values greater than 1.96 imply that locations within the specified radius are expected to be statistically similar ($\alpha = 0.05$) to nearby samples, a value less than -1.96 suggests statistically significant differences ($\alpha = 0.05$), and values between those represent a lack of statistical significance in either direction (Zhang and McGrath 2004; Sheppard et al. 2007). Ultimately, the minimum bandwidth is chosen by identifying the kernel radius at which the Moran's I value is maximized and the Z score is greater than 1.96.

3. Results

The K-means cluster analysis produced four days [day of year (DOY)] delineating seasons that seem to represent the annual tornado patterns appropriately (Table 1). Four seasons were produced with only three clusters because the fall and spring seasons are part of the same cluster (i.e., similar characteristics), but they are

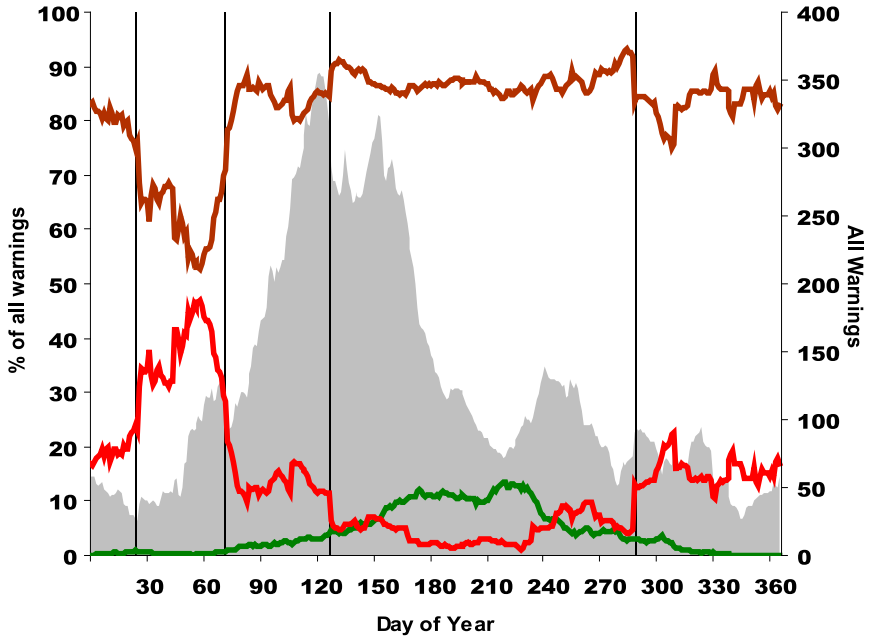

Figure 3. Vertical black bars show seasonal breaks based upon the results of cluster analysis. The green line is slow storms, the brown line is intermediate storms, and the red line is fast storms. The gray shading shows the total number of warnings per day of year for the study period.

temporally separated by winter and summer (Figure 3). These delineation times make for a rather long summer season, but allowing for a fourth cluster created two more breaks on DOY 155 (4 June) and DOY 239 (27 August), which would have created a "May season" and a "September season." With no clear justification for choosing one result over the other, the three-cluster method is used for the rest of this study because of its simplicity (i.e., four seasons).

It should be noted that the season-defining cluster analysis was also performed for the years 2001–10 simply to examine whether the historic activity of 2011 was significantly altering the results. All periods were identical between the two analyses with the exception of the spring–summer transition. The shorter analysis period yielded a summer beginning of DOY 100 (10 April), but the addition of

Table 2. Moran's I and *Z*-score values for various radii during the winter season using the two methods described in the methods section. Bold values show the first statistically significant (*Z* score > 1.96) peak in Moran's I.

East of 105°W			Tornado-prone states		
Radius (km)	Moran's I	*Z* score	Radius (km)	Moran's I	*Z* score
160	0.0348	13.73	150	0.0035	1.20
170	0.0340	14.21	160	0.0052	1.74
180	**0.0354**	**15.56**	170	0.0055	1.94
190	0.0336	15.57	**180**	**0.0080**	**2.81**
200	0.0319	15.55	190	0.0070	2.65

Table 3. As in Table 2, but for the spring season.

East of 105°W			Tornado-prone states		
Radius (km)	Moran's I	*Z* score	Radius (km)	Moran's I	*Z* score
150	**0.0204**	**27.30**	85	0.0225	16.95
160	0.0200	28.41	**90**	**0.0227**	**18.04**
170	0.0191	28.85	95	0.0224	18.74
180	0.0184	29.46	100	0.0225	19.79
190	0.0183	30.77	105	0.0221	20.42

2011 and 2012 shifted that day to DOY 128 (8 May). This suggests that the relatively short study period is not necessarily allowing for a clear delineation between the consistently fast-moving storms during spring and consistently slow-moving storms of summer. However, the consistency of the other seasons suggests that the method is useful.

Moran's I and *Z*-score values suggest varying ideal smoothing radii for each season and method (Tables 2–6). Analyses of all U.S. locations east of 105°W yield larger radii, but this result is likely due to the limitation introduced by spatial outliers. Nevertheless, the range of radii is rather small with values as low as 55 km (spatially restricted method for the fall season) and as high as 180 km (both methods for the winter season). Tornado path (and point) density maps were created using the full period of tornado data (1950–2011) and an Epanechnikov (bounded normal distribution) kernel (Dixon et al. 2011; Marsh and Brooks 2012; Smith et al. 2012) with the various radii for each season (Figures 4–7). The two different methods for including tornado paths (described in section 2.4) yielded different radii for all seasons but winter (Tables 2–5). For the density calculation of annual tornado initiation points (Figure 8), only the first method was used (Table 6).

Figures 4–7 illustrate the times of the year when U.S. locations are most at risk for tornadoes. This allows each location to establish its own annual period of preparedness, which may not be consistent with the widely publicized spring tornado season. In particular, many locations in the northern Great Plains and Midwest are more likely to experience tornadoes during our summer season, and some locations in the Deep South have a tornado season that runs continuously from the fall through the spring.

4. Conclusions

Despite the colloquial use of the term "Dixie Alley," Dixon et al. (Dixon et al. 2011) argue that the region of greatest tornado frequency and density in the United

Table 4. As in Table 2, but for the summer season.

East of 105°W			Tornado-prone states		
Radius (km)	Moran's I	*Z* score	Radius (km)	Moran's I	*Z* score
150	**0.0155**	**45.57**	**110**	**0.0143**	**29.44**
160	0.0150	47.00	115	0.0142	30.49
170	0.0146	48.33	—	—	—
180	0.0144	50.39	—	—	—
190	0.0140	51.48	—	—	—

Table 5. As in Table 2, but for the fall season.

East of 105°W			Tornado-prone states		
Radius (km)	Moran's I	*Z* score	Radius (km)	Moran's I	*Z* score
150	**0.0365**	**24.97**	**55**	**0.0180**	**3.64**
160	0.0340	25.63	60	0.0173	3.79
170	0.0351	26.19	—	—	—
180	0.0328	26.77	—	—	—
190	0.0317	27.31	—	—	—

States cannot be objectively separated into smaller ''alleys.'' It is understandable that people want to make this separation for a number of reasons, including the real and perceived differences in tornado speed, seasonality, diurnal timing, and fatalities across the country. Such spatial delimiters imply that certain locations tend to be grouped with other locations regardless of the time of year, and this also has the potential to lead the general public to overlook how tornado season varies with space. The results of this study may provide some help with this goal as the objective separation of the year into four tornado seasons allows locations to be included in the elevated risk area multiple times throughout the year. Hence, while one area may be considered ''different'' from another region during the fall or winter, they may be relatively similar during spring. Further, it helps to illustrate that one location may experience a significantly different ''tornado year'' than other locations. Ideally, researchers would be able to calculate minimum smoothing radii and tornado risk values separately for every day of the year, but that would require several thousand years of observations, assuming similar tornado frequencies to those over the past few decades. Therefore, the use of seasonal risk regions should remain a useful tool in the foreseeable future. It is also important to note that every state has experienced tornadoes, so no location is totally excluded from tornado risk, even if they are not highlighted by any of the maps provided here.

The ideal kernel radii suggested by this research are mostly within the ranges used by previous studies (Thom 1963; Kelly et al. 1978; Schaefer et al. 1986; Brooks et al. 2003; Dixon et al. 2011). The spatially restricted method used in this study produced a radius of 55 km for the fall season, and that yields a little less smoothing than any of the methods applied in the studies cited above. However, an argument can be made that a radius produced by our study acts more like a ''minimum'' rather than the universal ''ideal'' simply because even the maximum Moran's I values are quite low and *Z*-score values will remain statistically significant with increasing radii. Seasonal differences using any radii are much more

Table 6. Moran's I and *Z*-score values for various radii using tornado initiation points for the entire year. Bold values show the first statistically significant (*Z* score > 1.96) peak in Moran's I.

Radius (km)	Moran's I	*Z* score
70	**0.0366**	**88.31**
75	0.0356	91.72
80	0.0353	96.52
85	0.0348	100.92

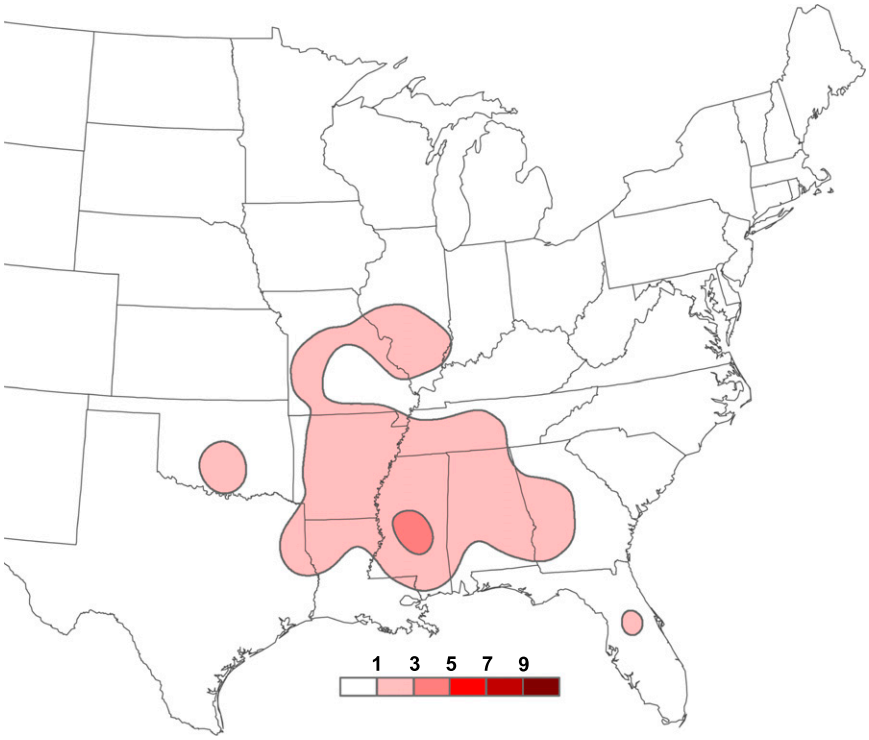

Figure 4. Kernel density estimations of annual winter tornado paths (km) within 40 km of a point using a 180-km bandwidth.

obvious than those created with different kernel bandwidths for the same season. Hence, spatial smoothing of tornado frequency or density maps may range widely, depending upon the intended purpose of the research, but the results of this study suggest that there are objective minima depending upon the characteristics of the

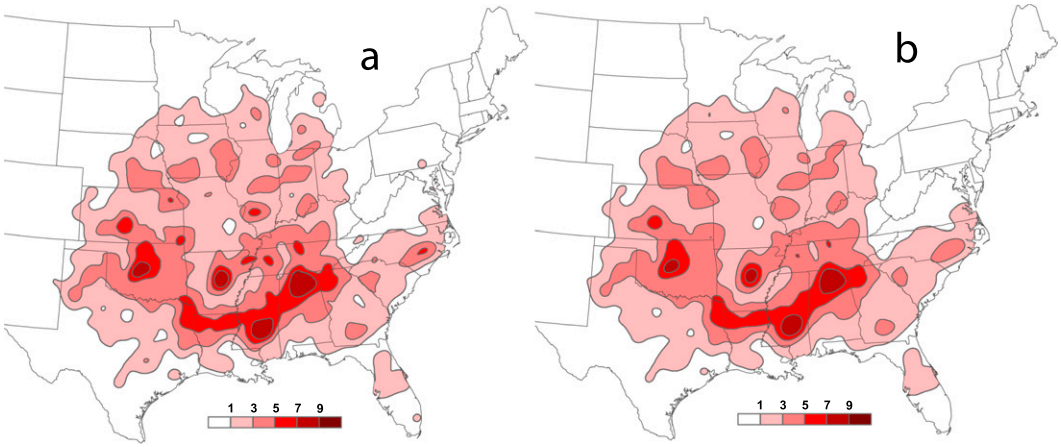

Figure 5. Kernel density estimations of annual spring tornado paths (km) within 40 km of a point using bandwidths of (a) 90 and (b) 150 km.

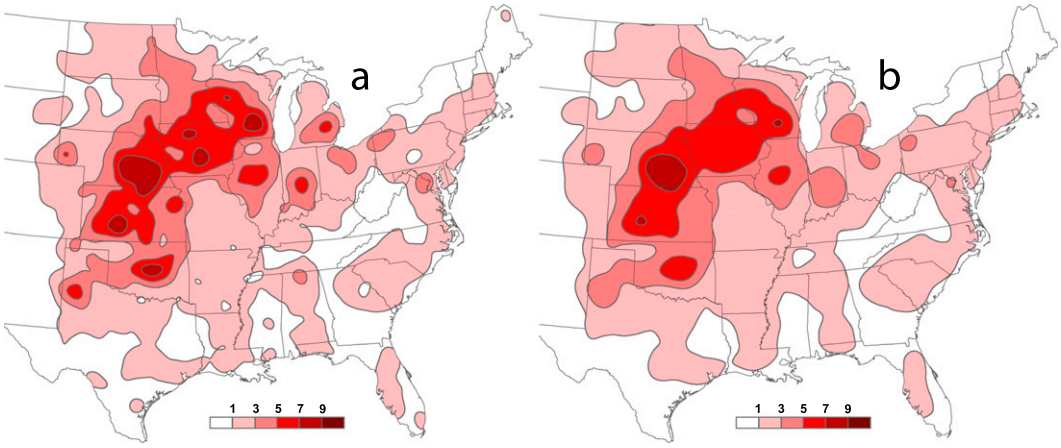

Figure 6. Kernel density estimations of annual summer tornado paths (km) within 40 km of a point using bandwidths of (a) 110 and (b) 150 km.

data being used to assess spatial autocorrelation [i.e., pathlength, enhanced Fujita (EF) scale, time of day, etc.]. These minima are likely to vary most, depending upon study period (both intra-annual and interannual), as there are clear differences in tornado characteristics and distributions by season and the current tornado dataset is not complete enough to ensure that samples from different periods are consistent.

While it may be argued that each season has a different minimum kernel bandwidth, it is important to apply consistency between seasons for the purposes of interpretation by nonexperts. Therefore, we recommend a radius of at least 150 km be applied in most applications simply because three of the four seasons yielded that bandwidth as the minimum when analyzing all data east of the Rocky Mountains (105°W longitude). This is also recommended because there are no

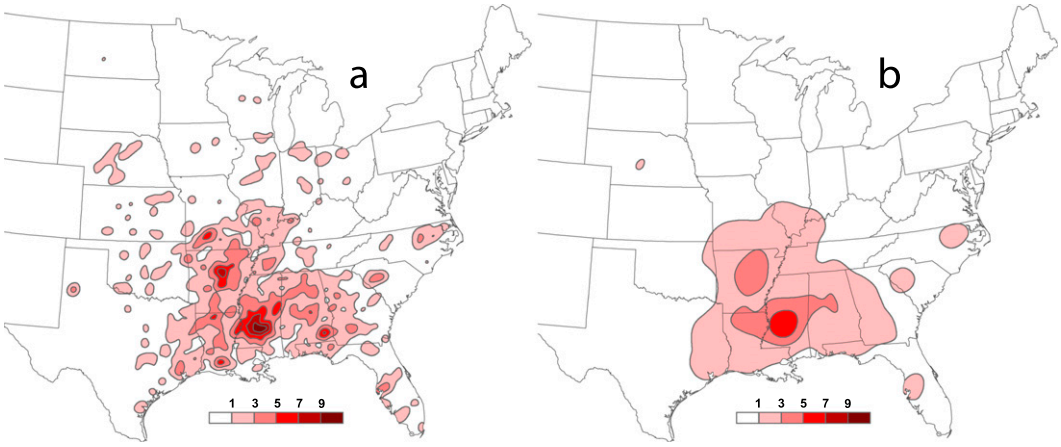

Figure 7. Kernel density estimations of annual fall tornado paths (km) within 40 km of a point using bandwidths of (a) 55 and (b) 150 km.

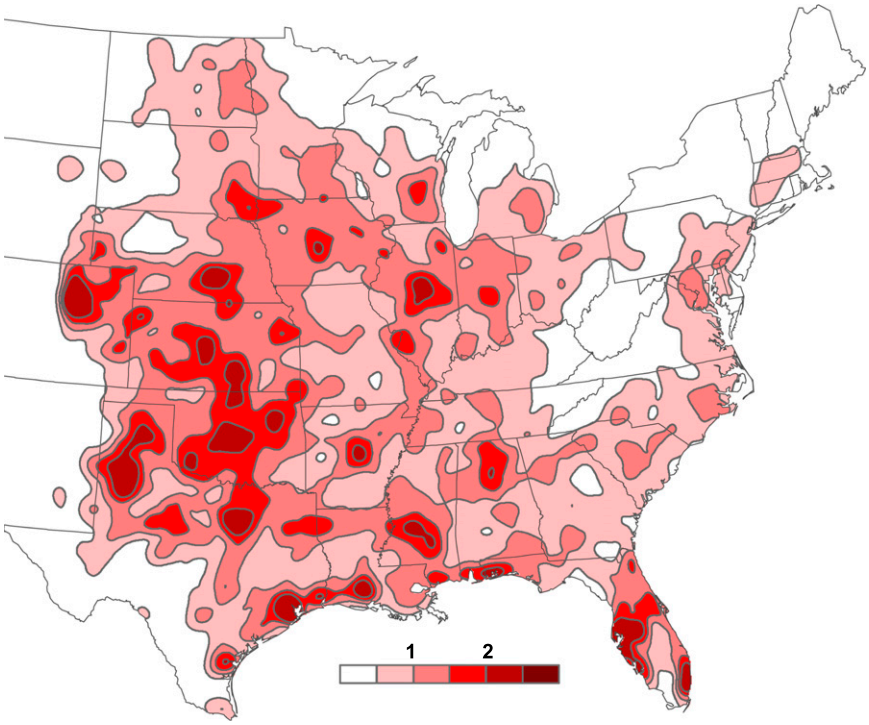

Figure 8. Kernel density estimations of total annual tornado initiation points per decade within 40 km of a point using a 70-km bandwidth.

objective reasons to exclude the ''spatial outliers'' in most cases. Perhaps another justified method is to use a ''lowest common radius'' of 180 km due to the minimum winter bandwidth, but the differences between 150- and 180-km radii should be minimal. Further, the ideal radii suggested here might be interpreted as the ideal ''effective radius'' for unbounded smoothing functions (e.g., Gaussian). For regional studies with small spatial extents, large distances between spatial outliers are less likely, so the smaller minimum radii may be applied. The opposite is true for shorter study periods. While the spatial patterns should remain consistent, it is important to note that various shapes of smoothing functions can yield different density magnitudes (Dixon and Mercer 2012; Marsh and Brooks 2012).

References

Anselin, L., 1995: Local indicators of spatial association—LISA. *Geogr. Anal.,* **27,** 93–115.

——, 1996: The Moran scatterplot as an ESDA tool to assess local instability in spatial association. *Spatial Analytical Perspectives on GIS,* M. Fischer, H. J. Scholten, and D. J. Unwin, Eds., Taylor & Francis, 111–115.

Ashley, W. S., 2007: Spatial and temporal analysis of tornado fatalities in the United States: 1880-2005. *Wea. Forecasting,* **22,** 1214–1228.

——, A. J. Krmenec, and R. Schwantes, 2008: Vulnerability due to nocturnal tornadoes. *Wea. Forecasting,* **23,** 795–807.

Boruff, B. J., J. A. Easoz, S. D. Jones, H. R. Landry, J. D. Mitchem, and S. L. Cutter, 2003: Tornado hazards in the United States. *Climate Res.,* **24,** 103–117.

Brooks, H. E., 2004: On the relationship of tornado path length and width to intensity. *Wea. Forecasting,* **19,** 310–319.

——, C. A. Doswell, and M. P. Kay, 2003: Climatological estimates of local daily tornado probability for the United States. *Wea. Forecasting,* **18,** 626–640.

Broyles, J. C., and K. C. Crosbie, 2004: Evidence of smaller tornado alleys across the United States based on a long track F3-F5 tornado climatology study from 1880-2003. Preprints, *22nd Conf. on Severe Local Storms,* Hyannis, MA, Amer. Meteor. Soc., P5.6. [Available online at https://ams.confex.com/ams/pdfpapers/81872.pdf.]

Concannon, P. R., H. E. Brooks, and C. A. Doswell III, 2000: Climatological risk of strong and violent tornadoes in the United States. *Proc. Second Conf. on Environmental Applications,* Long Beach, CA, Amer. Meteor. Soc., 212–219.

de Smith, M. J., M. F. Goodchild, and P. A. Longley, 2007: *Geospatial Analysis: A Comprehensive Guide to Principles, Techniques and Software Tools.* 3rd ed. Troubador, 516 pp.

Dixon, P. G., and A. E. Mercer, 2012: Reply to ''Comments on 'Tornado risk analysis: Is Dixie Alley an extension of Tornado Alley?''' *Bull. Amer. Meteor. Soc.,* **93,** 408–410.

——, ——, J. Choi, and J. S. Allen, 2011: Tornado risk analysis: Is Dixie Alley an extension of Tornado Alley? *Bull. Amer. Meteor. Soc.,* **92,** 433–441.

Doswell, C. A., III, 2007: Small sample size and data quality issues illustrated using tornado occurrence data. *E-J. Severe Storms Meteor.,* **2** (5), 1–16.

——, and D. W. Burgess, 1988: On some issues of United States tornado climatology. *Mon. Wea. Rev.,* **116,** 495–501.

Emery, S. C., 1900: Tornadoes in Tennessee, Mississippi, and Arkansas. *Mon. Wea. Rev.,* **28,** 499–501.

Fortin, M.-J., M. R. T. Dale, and J. ver Hoef, 2006: Spatial analysis in ecology. *Encyclopedia of Environmetrics,* A. H. El-Shaarawi and W. W. Piegorsch, Eds., John Wiley & Sons, 2051–2058.

Gagan, J. P., A. E. Gerard, and J. Gordon, 2010: A historical and statistical comparison of ''Tornado Alley'' to ''Dixie Alley.'' *Natl. Wea. Dig.,* **34,** 145–155.

Guyer, J. L., D. A. Imy, A. Kis, and K. Venable, 2006: Cool season significant (F2-F5) tornadoes in the Gulf Coast states. Preprints, *23rd Conf. on Severe Local Storms,* St. Louis, MO, Amer. Meteor. Soc., 4.2. [Available online at https://ams.confex.com/ams/pdfpapers/115320.pdf.]

Hanstrum, B. N., G. A. Mills, A. Watson, J. P. Monteverdi, and C. A. Doswell, 2002: The cool-season tornadoes of California and southern Australia. *Wea. Forecasting,* **17,** 705–722.

Kelly, D. L., J. T. Schaefer, R. P. McNulty, C. A. Doswell III, and R. F. Abbey, 1978: An augmented tornado climatology. *Mon. Wea. Rev.,* **106,** 1172–1183.

Kis, A. K., and J. M. Straka, 2009: Nocturnal tornado climatology. *Wea. Forecasting,* **25,** 545–561.

Marsh, P. T., and H. E. Brooks, 2012: Comments on ''Tornado risk analysis: Is Dixie Alley an extension of Tornado Alley?'' *Bull. Amer. Meteor. Soc.*

Marzban, C., and J. T. Schaefer, 2001: The correlation between U.S. tornadoes and Pacific sea surface temperatures. *Mon. Wea. Rev.,* **129,** 884–895.

McCarthy, D., 2003: NWS tornado surveys and the impact on the national tornado database. Preprints, *Symp. on the F-Scale and Severe-Weather Damage Assessment,* Long Beach, CA, Amer. Meteor. Soc., 3.2. [Available online at https://ams.confex.com/ams/pdfpapers/55718.pdf.]

Mitchell, M. S., and R. A. Powell, 2008: Estimated home ranges can misrepresent habitat relationships on patchy landscapes. *Ecol. Modell.,* **216,** 409–414.

Nelson, T. A., and B. Boots, 2008: Detecting spatial hot spots in landscape ecology. *Ecography,* **31,** 556–566.

O'Sullivan, D., and D. J. Unwin, 2003: *Geographic Information Analysis.* John Wiley & Sons, 436 pp.

Portnov, B. A., J. Dubnov, and M. Barchana, 2009: Studying the association between air pollution and lung cancer incidence in a large metropolitan area using a kernel density function. *Socio-Econ. Plann. Sci.,* **43,** 141–150.

Santamaría, L., J. Rodríguez-Pérez, A. R. Larrinaga, and B. Pias, 2007: Predicting spatial patterns of plant recruitment using animal-displacement kernels. *PLoS ONE,* **2,** e1008, doi:10.1371/journal.pone.0001008.

Schaefer, J. T., and R. Edwards, 1999: The SPC tornado/severe thunderstorm database. *Proc. 11th Conf. on Applied Climatology,* Dallas, TX, Amer. Meteor. Soc., 215–220.

——, D. L. Kelly, and R. F. Abbey, 1986: A minimum assumption tornado-hazard probability model. *J. Appl. Meteor.,* **25,** 1934–1945.

Sheppard, J. K., I. R. Lawler, and H. Marsh, 2007: Seagrass as pasture for seacows: Landscape-level dugong habitat evaluation. *Estuar. Coastal Shelf Sci.,* **71,** 117–132.

Smith, B. T., R. L. Thompson, J. S. Grams, C. Broyles, and H. E. Brooks, 2012: Convective modes for significant severe thunderstorms in the contiguous United States. Part I: Storm classification and climatology. *Wea. Forecasting,* **27,** 1114–1135.

Thom, H. C. S., 1963: Tornado probabilities. *Mon. Wea. Rev.,* **91,** 730–736.

Wilks, D. S., 2006: *Statistical Methods in the Atmospheric Sciences.* 2nd ed. Academic Press, 467 pp.

Willems, E. P., and R. A. Hill, 2009: Predator-specific landscapes of fear and resource distribution: Effects on spatial range use. *Ecology,* **90,** 546–555.

Wood, V. T., R. A. Brown, and D. W. Burgess, 1996: Duration and movement of mesocyclones associated with southern Great Plains thunderstorms. *Mon. Wea. Rev.,* **124,** 97–101.

Zhang, C., and D. McGrath, 2004: Geostatistical and GIS analyses on soil organic carbon concentrations in grassland of southeastern Ireland from two different periods. *Geoderma,* **119,** 261–275.